Fish and Shellfish Immunology 93 (2019) 416–427

Contents lists available at ScienceDirect

Fish and Shellfish Immunology

journal homepage: www.elsevier.com/locate/fsi

Full length article

Molecular characteristics of AMPK and its role in regulating the phagocytosis of oyster hemocytes

Zhiying He[a,b], Fan Mao[a], Yue Lin[a,b], Jun Li[a], Xiangyu Zhang[a,b], Yuehuan Zhang[a], Zhiming Xiang[a], Zohaib Noor[a,b], Yang Zhang[a,*], Ziniu Yu[a,**]

[a] Key Laboratory of Tropical Marine Bio-resources and Ecology, Guangdong Provincial Key Laboratory of Applied Marine Biology, Institution of South China Sea Ecology and Environmental Engineering, South China Sea Institute of Oceanology, Chinese Academy of Science, Guangzhou, 510301, China
[b] University of Chinese Academy of Sciences, Beijing, 100049, China

ARTICLE INFO

Keywords:
AMPK signaling
Crassostrea hongkongensis
Phagocytosis
Hemocytes
Compound C

ABSTRACT

Phagocytosis is one of the fundamental cellular immune defense parameter that helps in the elimination of the invading pathogens in both vertebrates and invertebrates, which require plenty of energy for functioning. In the present study, we identified the critical energy regulator AMP-activated protein kinase (AMPK) in *Crassostrea hongkongensis* which is composed of three subunits, named *Ch*AMPK-α, *Ch*AMPK-β, and *Ch*AMPK-γ, and then analyzed the function of AMPK in regulating hemocyte phagocytosis. All the three *Ch*AMPK subunits mRNA were detected to be expressed at various embryological stages, and also constitutively expressed in multiple tissues with high expression in gill and mantle. The phylogenetic tree showed that the three subunits of AMPK were correspondingly clustered with its orthologue branches. Furthermore Western Blot analysis revealed that the AMPK pharmacological inhibitors Compound C could effectively down-regulate the Thr^{172} phosphorylation level of AMPK-α, and the hemocyte phagocytosis was inhibited by Compound C (CC), which indicate its existence in the oyster. Our results showed that treatment of AMPK inhibitors significantly attenuated the capacity of hemocytes phagocytosis. Moreover, Compound C could also change the organization of actin cytoskeleton in the oyster hemocytes, demonstrating the crucial role of AMPK signaling in control of phagocytosis.

1. Introduction

AMP-activated protein kinase (AMPK) is a highly evolutionary conserved serine/threonine kinase, which is found in various species from yeast (SNF1) to plants (SnRK1) to humans [1]. As a conserved signaling molecule, mammalian AMPK was initially discovered in independent studies as protein kinase derived from the rat liver [2]. AMPK was given its name by the author in 1988 [3]. The AMPK of vertebrates is heterotrimeric kinase composed of catalytic α subunit and two regulatory subunits, β and γ [4]. AMPK subunits have distinct expression pattern in different tissues of mammals, which contain two α subunits (α1, α2), two β subunits (β1, β2), and three γ subunits (γ1, γ2 and, γ3) [5]. Two or three genes encoding each subunit resulting in 12 possible heterotrimeric combinants, and spliced variants further enhance the potential [6].

The AMPK three subunits have a similar domain structure in all eukaryotes. The main functional component of the AMPK complex is the catalytic α subunit (AMPK-α). Many studies [7,8] demonstrate that AMPK-α includes one serine/threonine kinase domain (KD), one auto inhibitory domain (AID), and one β binding domain (α-CTD). The kinase domain (KD) determines the kinase activity of the complex, which has Thr^{172} or Ser^{483} phosphorylation sites [9]. The AID domain has the ability to suppress the catalytic activity of AMPK [10]. AMPK-β contains a C-terminal region (β-CTD) required for the association with α and γ subunits and a central region (GBD) that allows the AMPK complex to bind glycogen [11]. A previous study showed that the β subunits act as targeting scaffolds that influence subcellular localization [12]. Almost in all species, AMPK-γ subunits contain a core nucleotide-binding module that is made up of four cystathionine-β-synthase (CBS) domains [13]. Under lowered intracellular ATP levels, a conformational

* Corresponding author. South China Sea Institute of Oceanology, Chinese Academy of Sciences, 164 West Xingang Road, Guangzhou, 510301, China.
** Corresponding author. South China Sea Institute of Oceanology, Chinese Academy of Sciences, 164 West Xingang Road, Guangzhou, 510301, China.
E-mail addresses: yzhang@scsio.ac.cn (Y. Zhang), carlzyu@scsio.ac.cn (Z. Yu).

https://doi.org/10.1016/j.fsi.2019.07.075
Received 20 March 2019; Received in revised form 20 July 2019; Accepted 26 July 2019
Available online 30 July 2019

Table 1
The sequences of the designed primers used in this study.

Primer	Sequence (50–3′)	Comment
ORF-Ampk-alpha-F	TTCAGTTCGTCTGTGTCCTT	ORF
ORF-Ampk-alpha-R	GTTCTTCATTTCTGGCATTC	ORF
ORF-Ampk-beta-F	TGATGTTCAGTGTCCTCGTTT	ORF
ORF-Ampk-beta-R	CGTCATTCCCTTCCCGTAT	ORF
ORF-Ampk-gamma-F	AACACTCCCCCTCCACATCCGC	ORF
ORF-Ampk-gamma-R	AACCGCACTGGGGGGTCCGAT	ORF
q-Ampk-alpha-F	GGTGATGGAGTATGTGTCTGG	Real time RT-PCR
q-Ampk-alpha-R	TAGGAGGAGGTTTTCTGGTTT	Real time RT-PCR
q-Ampk-beta-F	CTCCCTCACCGCTGGTAGATT	Real time RT-PCR
q-Ampk-beta-R	TTTCCTCCACCTTCCCATTTA	Real time RT-PCR
q-Ampk-gamma-F	AACACTCCCCCTCCACATCCG	Real time RT-PCR
q-Ampk-gamma-R	CTCCCCCAGGCGGACTACACT	Real time RT-PCR
Race Ampk-alpha- R1	GAGAATCTTTACCGCCACCTT	5′RACE
Race Ampk-alpha- R2	ATCTTGACTTGTGCGTTTTGA	5′RAC
Race Ampk-alpha- F1	GGTCATCCTGTATGCCTTGC	3′RACE
Race Ampk-alpha- F2	TGGGGTGACAGAGTATGAGGTA	3′RACE
Race Ampk-beta- R1	GGAATCTACCAGCGGTGAGGG	5′RACE
Race Ampk-beta- R2	GGCAGCCGTATCTCCTTGACT	5′RAC
Race Ampk-beta- F1	ATTCTACCTCCCCATCTGCTA	3′RACE
Race Ampk-beta- F2	ATGCTAAATCATCTGTATGCCTTGT	3′RACE
Race Ampk-gamma-R1	ACTTTTCACTTTGGCGGATGT	5′RACE
Race Ampk-gamma-R2	TTTGGCACTGTGATGTCGTTT	5′RACE
Race Ampk-gamma-F1	CGTCCAATGCCAATGAACCAA	3′RACE
Race Ampk-gamma-F2	ACACTCATGCAATCATCTACAAATC	3′RACE

Primers used in this study. “F” indicates forward primer and “R” indicates reverse primer.

change occurs via AMP or ADP directly bind to the γ regulatory subunits to protect the activating phosphorylation of AMPK [14]. Currently, the most distinct mechanisms of AMPK activation are phosphorylation at Thr^{172} of the α-subunit and by AMP and/or adenosine diphosphate (ADP) binding to γ subunit [15].

In invertebrates, the phagocytes are likely to undertake significant roles in immune defense, which are lacking canonical adaptive immunity and mainly rely on the innate immune system to fight against pathogens [16]. Phagocytosis is defined as the mechanism of internalization of large particulates material that is approximately 0.5μm or greater [17,18]. Phagocytosis is considered as an early and fundamental step for the effective eradication of disease-causing agents. Oysters are marine bivalve, belongs to the phylum Mollusca which is the second largest phylum of the animal kingdom, cultured worldwide and have great economic value. It is generally considered that oysters only possess innate immunity [19], while phagocytosis is considered as the vital parameter of it, which play a crucial role in the host defense of oyster, which is performed by circulating hemocytes [20].

The previous studies reported the homolog of AMPK, which has been identified in several invertebrates species, including *Brachytrupes orientalis* [21], Artemia [22], rock crab [23], a nemertean worm [24] and Mussels [25]. However, it is still unclear whether AMPK is associated with the hemocytes phagocytosis in the invertebrate. To address this issue, we cloned homolog of AMPK from the Hong Kong oyster, *Crassostrea hongkongensis*, which is one of local commercially valuable aquaculture species that thrive along the coast of South China Sea [26]. The present study is a giant leap in this regard, we also characterized its expression profile, and ability in the regulation of phagocytosis and actin cytoskeleton, which will benefit us for understanding the molecular signaling control of the oyster immune defense.

2. Materials and methods

2.1. Animals, tissue, embryonic development and immune challenge sample collection

The two years old Hongkong oysters from Zhanjiang, Guangdong Province, China, were stocked in the fiberglass Aquaria supplied with recirculating seawater (salinity of 20‰) for 3–7 days before the experiment. The oysters were fed twice a day with *Tetraselmis suecica* and *Isochrysis galbana*.

To analyze the distribution of three *Ch*AMPK genes in the different tissues, samples were obtained from the healthy Hongkong oysters including gill, mantle, heart, labial palps, adductor muscles, digestive glands, gonads and hemocytes. Three individuals of oysters were pooled for one samples, and three replications were carried out for each tissue. Samples from the developmental stages were also collected including the fertilized egg, 2 cells, blastula stage, gastrula, trochophore, veliger and eyespot larvae. Three individuals were pooled for one samples, and three replications were carried out for each developmental stages. An *in vivo* infection experiment was performed according to our previous work [27]. Hemocytes from both challenged and control group were sampled at 3, 6, 12 and 24 h post-injection. Three individuals were pooled for one samples, and three replications were carried out for each time point. Each sample was homogenized adequately in 1 mL of TRIzol for RNA extraction and was stored at −80 °C until further analysis.

2.2. RNA extraction and cDNA synthesis

Total RNA was isolated from the frozen tissue using TRIzol Reagent (Invitrogen, USA) according to the manufacturer's protocol. The integrity of RNA and the RNA concentration were checked with agarose gel electrophoresis and the absorbance pattern at 260 and 280 nm. Purified RNA sample was diluted to 1 mg/mL to perform cDNA synthesis using PrimerScript™ First Strand cDNA Synthesis kit (TAKARA Bio Inc. Japan) following the manufacturer's protocol.

2.3. Full-length cloning of three ChAMPK subunits

According to partial *Ch*AMPK sequences retrieved from *C. hongkongensis* transcriptome database, the full length of *Ch*AMPK was obtained using the SMART-RACE™ kit (Clontech, Japan) following the manufacturer's instructions. All the primers used are listed in Table 1.

Fig. 1. Sequence analysis of *Ch*AMPK-α. Full sequence and deduced amino acid sequences of *Ch*AMPK. The number on the left is for the nucleotide and amino acid order. The start (ATG) and stop (TAG) codons are presented in bold and underlined. Black framed and shaded regions represent kinase domains, only shadows represent β binding domain (α-CTD).

Fig. 2. Sequence analysis of *Ch*AMPK-β. Full sequence and deduced amino acid sequences of *Ch*AMPK. The number on the left is for the nucleotide and amino acid order. The start (ATG) and stop (TAG) codons are presented in bold and underlined. Black framed and shaded regions represent β-CTD domains (amino acids 179–269), only shadows represent GBD domain (amino acids 71–157).

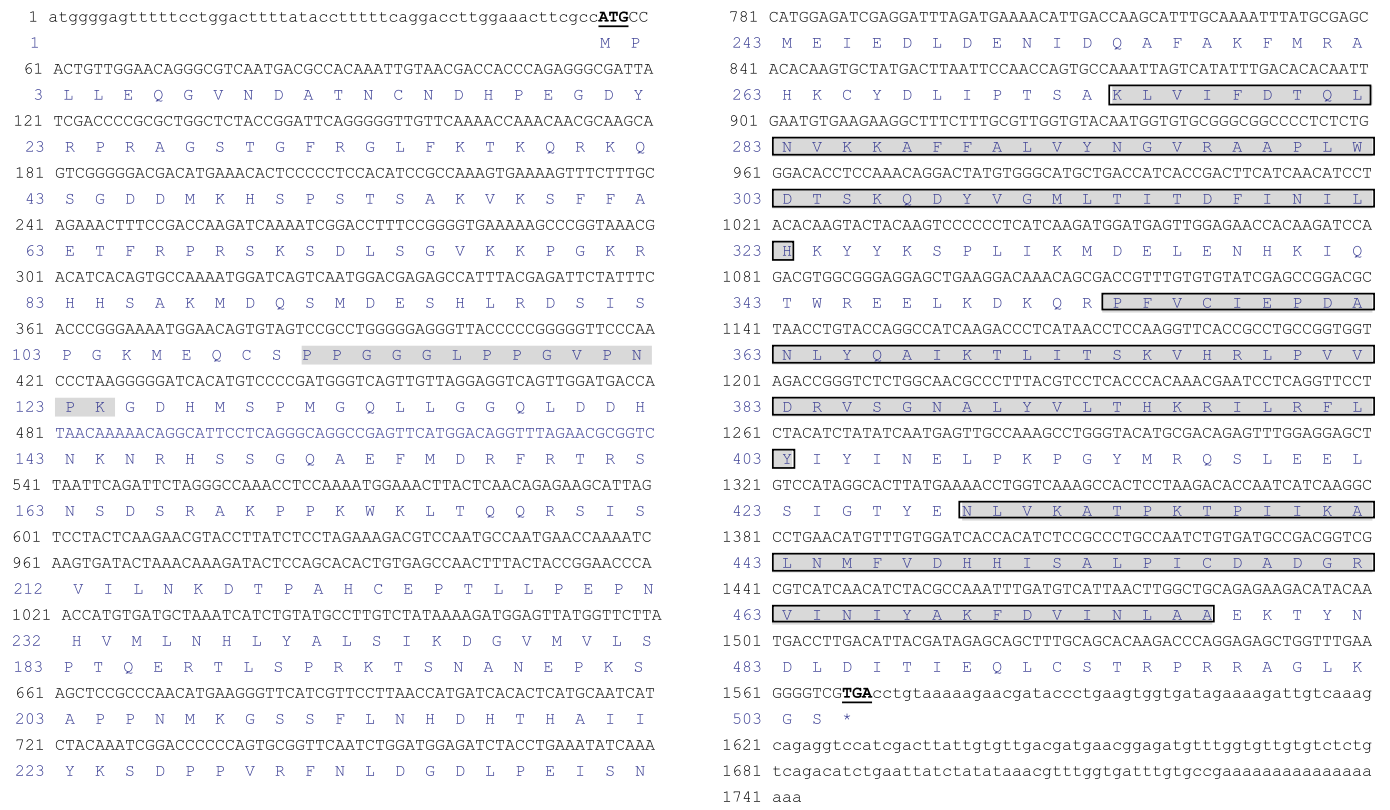

Fig. 3. Sequence analysis of *Ch*AMPK-γ. Full sequence and deduced amino acid sequences of *Ch*AMPK. The number on the left is for the nucleotide and amino acid order. The start (ATG) and stop (TAG) codons are presented in bold and underlined. Black framed and shaded regions represent CBS repeats, only shadows represent low compelxity domain.

2.4. Bioinformatics analysis of three ChAMPK subunits

The *Ch*AMPK subunits sequences were analyzed using the BLAST algorithm at NCBI (http://www.ncbi.nlm.nih.gov/blast), and the deduced amino acid sequence was obtained with the ORF finder (http://www.ncbi.nlm.nih.gov/gorf/orfig.cgi). Further, Protein motifs were predicted with SMART (http://smart.embl-heidelberg.de). A neighbor-joining (NJ) phylogenetic tree was constructed based on the amino acid sequences of known AMPK proteins using the MEGA version 7.0 with 1000 bootstrap replicates.

2.5. Expression pattern analyses of three ChAMPK subunits

The qRT-PCR was conducted using the 2 × RealStar Green Power Mixture Kit (GENE STAR, China) using the LightCycler 480II System (Roche, United States), according to the manufacturer's protocol. Each qRT-PCR analysis was performed in triplicate with GAPDH as an internal control, as it is a gene which is independent of tissue type and growth period. Besides, for each gene, the full sample under the same experimental treatment was run on the single plate to avoid any technical variation and inter-plate differences. The transcript quantifications of the genes were calculated using the using the $2^{-\Delta\Delta CT}$ method [28].

2.6. Total protein extraction

Hemocytes from Hongkong oysters were extracted and plated in 6-well cell plates, 500 μL per well, and cultured at 20 °C for 15 min. Then, the cells were observed under the microscope. The experimental group was treated with the AMPK inhibitor compound C (final concentration 50 μM). An equal amount of PBS was added to cells as the control group. After 3 h, the cells were resuspended in PBS with 15‰ EDTA solution and collected in a 1.5 mL centrifuge tube. After centrifugation at 12,000 rpm for 5 min at 4 °C, the pellet was lysed on ice for 30 min with IP Cell lysis Buffer (Biotech, product number: C500035) and vigorously shaken 3 times during the lysis. After centrifugation, the supernatant was collected, and the concentration was measured using BCA assay (Thermo, Prod# 23227). The protein was stored at −80 °C for the WB experiment.

2.7. Western blot analyses

Protein samples were denatured with 4 × SDS-loading buffer (200 mM Tris, pH 6.8, 8% SDS, 400 mM DTT, 0.4% bromphenol blue, 40% glycerol) at 99 °C for 10 min and subjected to standard SDS-PAGE and western blot analysis as previously described [29].

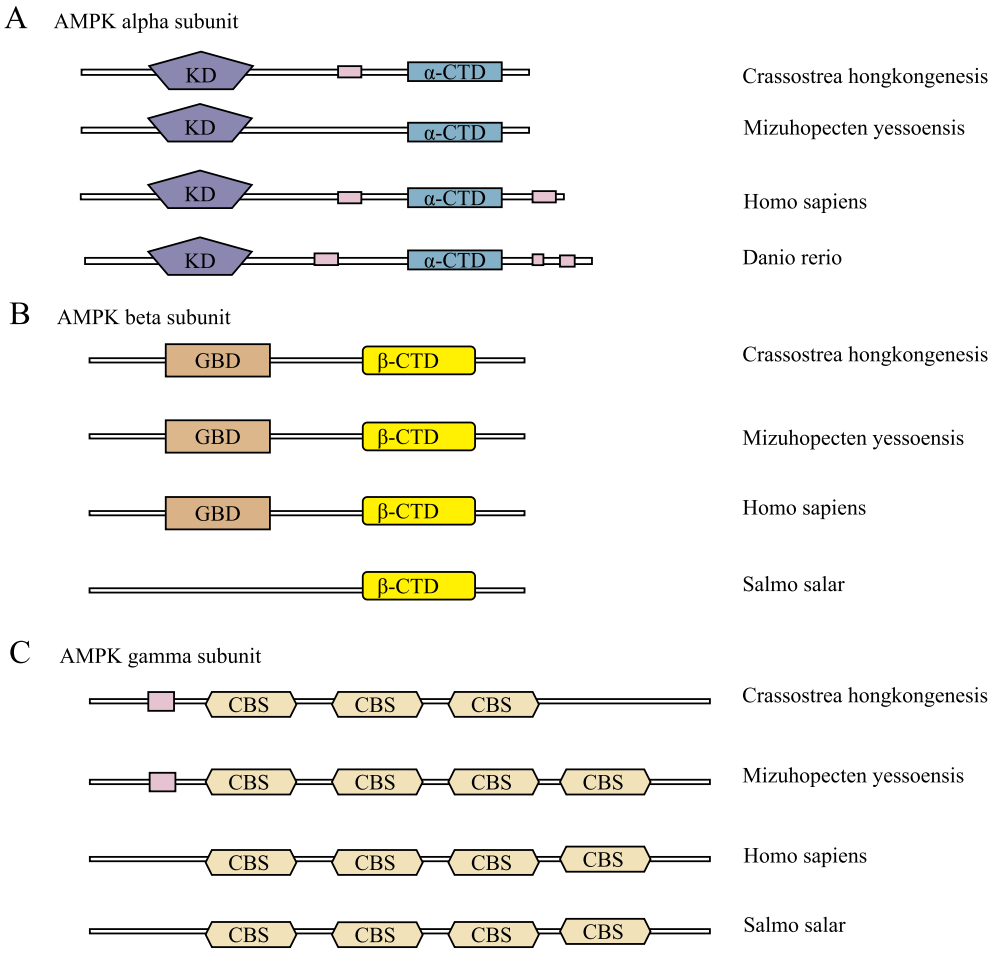

Fig. 4. Typical domain structure of AMPK. Typical domain structure of the α, β and γ subunits of *Ch*AMPK and its homologues in eukaryotes.

Immunodetection was performed with a rabbit monoclonal antibody anti-AMPK-α (dilution 1:1000; CST #2603) and a rabbit monoclonal antibody anti-phospho-threonine 172 AMPK-α (dilution 1:1000; CST #2535; Ozyme); Blots were then revealed using a horseradish peroxidase-linked secondary goat anti rabbit antibody (dilution 1:5000) and a horseradish peroxidase detection kit (Sangon Biotech). The relative amount of protein detected was quantified using ImageJ software with the background signal removed.

2.8. Flow cytometry analysis

Hemocyte were obtained by allowing 300 μL cells to adhere to individual wells (2–5 × 10^5 cells per well) of a 24-well culture plate at 20 °C for 15 min [30]. The experimental group was treated with the AMPK inhibitor CC (final concentration 50 μM) compared to the control group. After 30 min, fluorescent *E. coli* (C2566-EGFP; #8602678; Bio-Vector NTCC) was added in a ratio of 50:1 and incubated with the cells for 15 min. Then the cells were washed 3 times by Tris-HCl with 0.25% trypsin (pH 8.0, 50 mM) and resuspended with PBS with 15‰ EDTA. By using trypsin, non-internalized bacterial were removed from the cell membrane [31]. According to previous methods, hypothermia (4 °C) treatment could completely block phagocytosis but not affect the adhesion [32,33]. The same experiment was performed under 4° in order to detect adhesion rate. The cell aggregation was removed from the filtration membrane (REF 352235; 12 × 75 style; FALCON) and also checked under microscope (EVOS M5000, ThermoFisher). Flow cytometry was used to detect the phagocytosis of the oyster hemocytes, and at least 10,000 cells were collected. The results were analyzed using Flowjo software.

2.9. Laser confocal experiment

1 mL of hemocytes were plated in a glass bottom cell culture dish and incubated at 20 °C for 15 min. The experimental group was treated with the AMPK inhibitor CC (final concentration 50 μM) for 30 min. And an equal amount of PBS was incubated with the cells as the control group. Beads labeled with fluorescein isothiocyanate were added and incubated for 15 min in the dark. After fixing the cells with 4% paraformaldehyde, 0.1% X-100 was added, and the reaction was protected from light for 10 min then the cells were washed three times with PBS

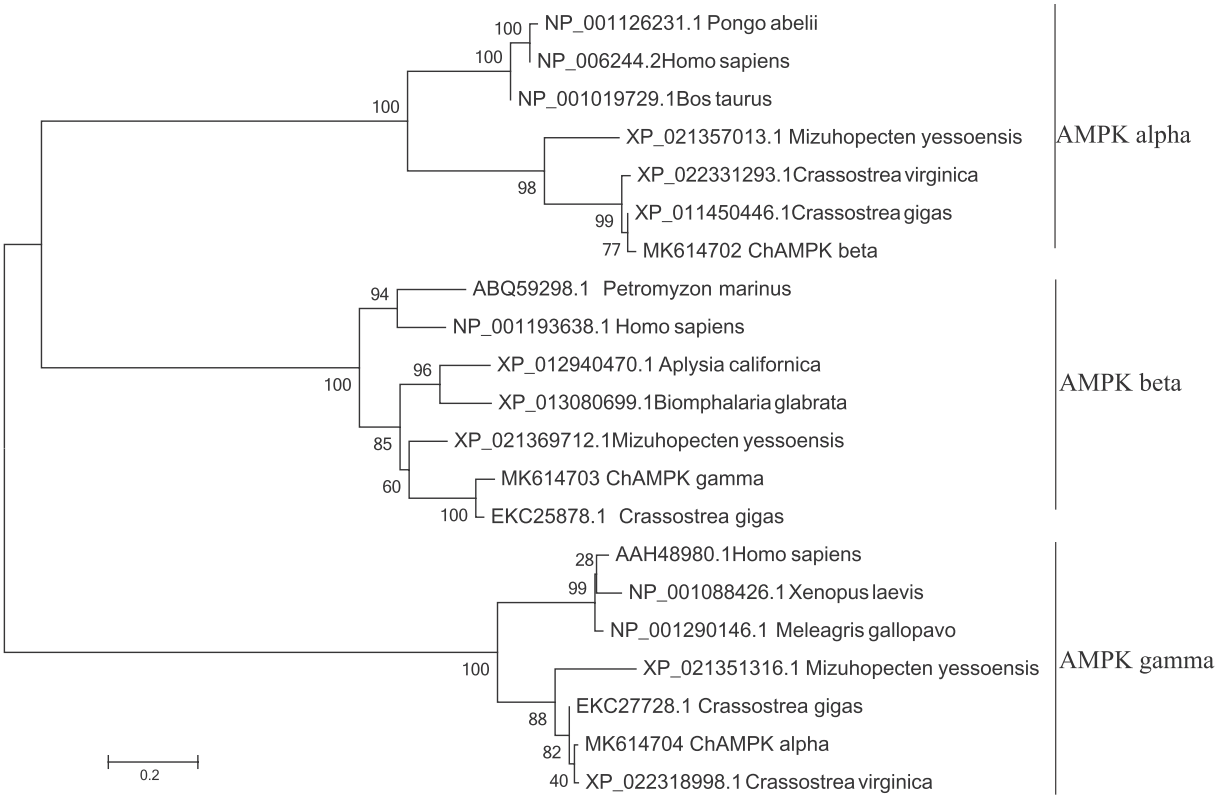

Fig. 5. Phylogenetic analysis of *Ch*AMPK. Phylogenetic tree analysis of the amino acid sequences of *Ch*AMPK protein and its homologs was constructed by the neighbor-joining (NJ) method and was bootstrapped 1000 times using the MEGA 5.0 software.

and incubated with ActinRed™ 555 for 30 min. Finally, DAPI (final concentration of 2.5 μg/μL) was added for 5 min. The experimental results were observed under a Laser Scanning Confocal Microscopy.

1 mL of hemocytes were plated in a glass bottom cell culture dish and incubated at 20 °C for 15 min. The experimental group was treated with the AMPK inhibitor CC (final concentration 50 μM) for 30 min. And an equal amount of PBS was incubated with the cells as the control group. After fixing the cells with 4% paraformaldehyde, 0.1% X-100 was added, and the reaction was protected from light for 10 min then the cells were washed three times with PBS and incubated with ActinRed™ 555 for 30 min. Finally, DAPI (final concentration of 2.5 μg/μL) was added for 5 min. The experimental results were observed under a Laser Scanning Confocal Microscopy.

2.10. Statistical analysis

All of the statistical analyses were carried out with SPSS 18.0 software. All data are presented as mean ± standard deviation (SD). The significant differences between groups were analyzed by one-way ANOVA followed by Turkey's multiple comparison tests. Significant differences are indicated by an asterisk (*, ** and ***represent $p < 0.05$, $p < 0.01$ and $p < 0.001$ respectively).

3. Results

3.1. Cloning and characterization of Hongkong oyster AMPK subunits

AMPK alpha subunit. The full-length *Ch*AMPK-α cDNA sequence obtained from Hongkong oyster was submitted to GenBank (accession number: MK614704). The length of the obtained complete cDNA sequence of *Ch*AMPK-α is 2099 bp, including a 206 bp 5′ untranslated region (UTR), a 1635 bp ORF, and a 258 bp 3′UTR。The ORF encodes a protein consisting of 544 amino acid residues with a calculated molecular mass of 45 kDa and a theoretical isoelectric point of 6.5 (Fig. 1). The conserved domains of *Ch*AMPK-α were predicted and analyzed by the SMART program, including one S-TKc domains (KD) and one autoinhibitory domain (AID) and one β binding domain (α-CTD), consistent with the typical features of AMPK-α family proteins (Fig. 4A).

AMPK beta subunit. A full length of 1705 bp encoding *Ch*AMPK-β was cloned from hemocyte cDNA library (GenBank accession number: MK614702). 329 bp and 566 bp nucleaic acid fragments were cloned as 5′ untranslated regions (UTR) and 3' UTR, respectively. An open reading frame (ORF) of 810 bp was characterized encoding a putative protein of 269 amino acid residues with a calculated molecular mass of 23 kDa and pI of 7.09. The complete nucleotide sequence and the deduced amino acid sequence of *Ch*AMPK-β are shown in Fig. 2. Smart program analysis characterized the *Ch*AMPK-β motifs in the predicted

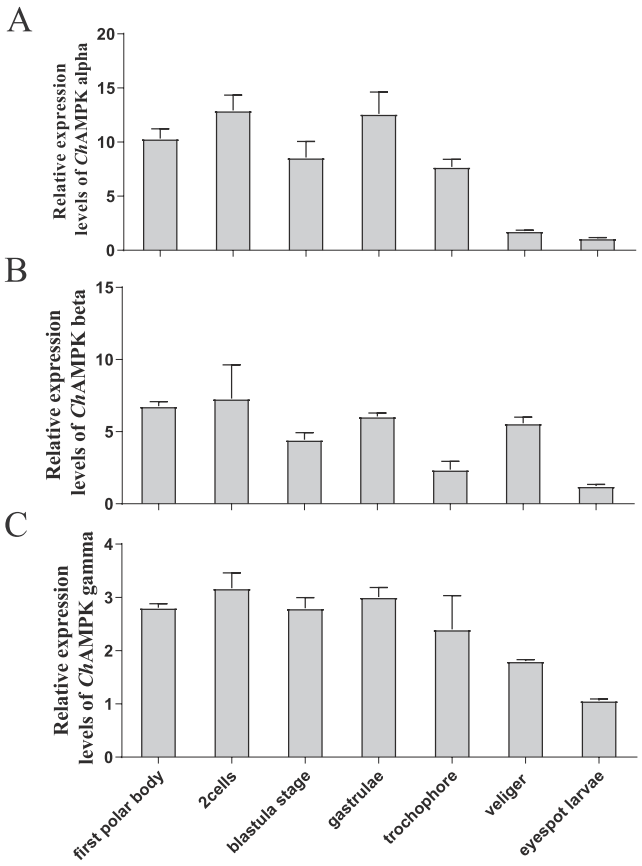

Fig. 6. Expression analysis of *Ch*AMPK in different embryonic stages. *Ch*AMPK mRNA expression during different embryonic stages: first polar body, second polar body, 2 cells, mulberry embryo, blastula stage, gastrula, trochophore, veliger and eyespot larvae. Each bar represents the mean of the normalized expression levels of the replicates (N = 3).

amino acid sequence. The GBD domain (amino acids 71–157) and β-CTD domains (amino acids 179–269) are conserved domain compared to the AMPK-β subunits of other species (Fig. 4B).

AMPK gamma subunit. Based Hong Kong Oyster Gene Transcriptome, one novel full-length of *Ch*AMPK-γ cDNA sequence, designated it as *Ch*AMPK-γ subunit, was obtained (Fig. 3) The complete cDNA sequence of *Ch*AMPK-γ consists of 1743 bp (GenBank accession number: MK614703), including an ORF of 1515 bp, a 55 bp 5′untranslated region (UTR), and a 173 bp 3′ UTR. The ORF encodes a putative 504 amino acid protein, with a predicted molecular weight of 40 kDa. Similar to other AMPK-γ proteins, *Ch*AMPK-γ contains the conserved domains, CBS repeat (Fig. 4C).

3.2. Phylogenetic analysis of ChAMPK

The phylogenetic tree was built based on AMPK protein sequences from *C. hongkongensis* and other species using MEGA6.0 software. As shown in Fig. 5, the evolutionary tree reveals three main clusters corresponding to the three different families of AMPK, which indicates that *Ch*AMPK and *C. gigas* AMPK have the closest evolutionary relationship

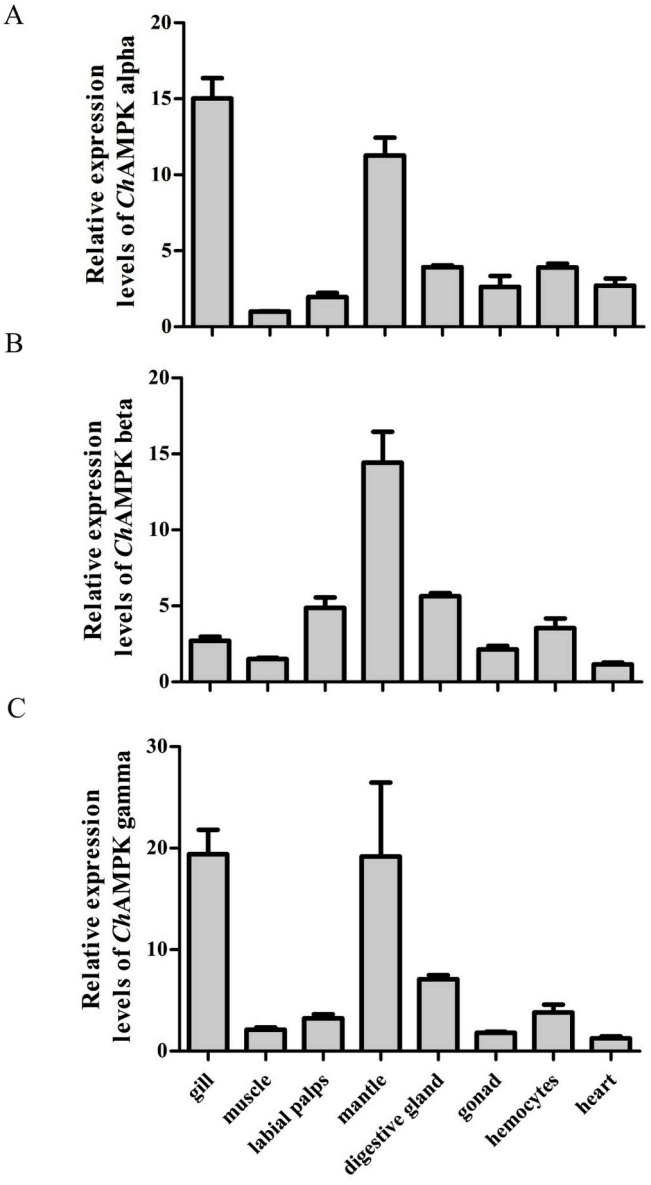

Fig. 7. Expression profile of *Ch*AMPK mRNA in different tissues. mRNA expression of *Ch*AMPK in different tissues determined by quantitative real-time PCR. GAPDH gene expression was used as an internal control. Vertical bars represent the mean ± SE (N = 3).

(supported by 1000 bootstrap).

3.3. Expression pattern of ChAMPK

The mRNA expression pattern of *Ch*AMPK was detected via qRT-PCR. The results showed that three *Ch*AMPK subunits expressed at all developmental stages. The expression of all *Ch*AMPK subunits from fertilized eggs to trochophores was relatively high, while the expression of *Ch*AMPK-α and *Ch*AMPK-γ were considerably lower in the veliger larvae (Fig. 6).

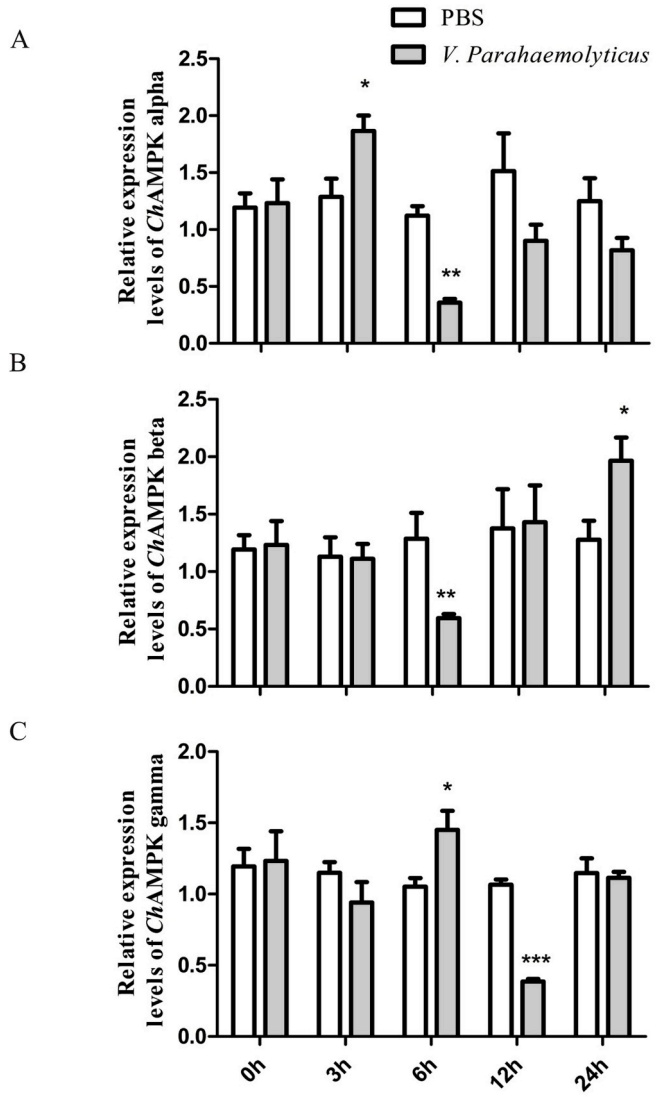

Fig. 8. *Ch*AMPK mRNA expression after bacterial challenge in hemocytes. *Ch*AMPK mRNA expression was evaluated at 0 h, 3 h 6 h, 12 h and 24 h after exposed to *Vibrio parahaemolyticus*, which was calculated by the $2^{-\Delta\Delta CT}$ method using GAPDH as the internal control. Error bar represents the means ± SE (N = 3). *, $p < 0.05$, **,$p < 0.01$, ***, $p < 0.001$.

Fig. 7 showed that *Ch*AMPK-α, *Ch*AMPK-β and *Ch*AMPK-γ widely expressed in all tissues, including heart, muscle, hemocytes, mantle, digestive gland, gonads and gills. *Ch*AMPK-α highly expressed in the gill and mantle. And the lowest expression of *Ch*AMPK-α can be observed in muscle. The expression of *Ch*AMPK-β was higher in the digestive glands and mantle, as these two tissues are considered as the immune organs of oysters. The expression level of *Ch*AMPK-γ was high in the gills, followed by muscles and gonad while lowest expression was observed in the heart.

3.4. Time-dependent expression of ChAMPK after immune stimulation

The temporal expression profile of *Ch*AMPK in hemocytes following bacterial challenge was also investigated (Fig. 8). The expression of *Ch*AMPK-α was up-regulated after 3 h bacterial stimulation compared with the control group, and it decreased to a significantly low level at 12 h post injection. After immunostimulation, the expression level of *Ch*AMPK-β gene was significantly lower than that of the control group at 6 h. However, compared with the control group, the mRNA expression level of *Ch*AMPK-γ reached a peak at 6 h post-challenge, and the lowest expression was observed at 12 h post injection.

3.5. AMPK-α protein and phosphorylation level under compound C treatment

To investigate the inhibitory effect of Compound C on AMPK signaling, western blot analysis was performed for the detection of total and phosphorylation level of *Ch*AMPK-α protein. As shown in Fig. 9A, the bond size for *Ch*AMPK-α protein is at 45 kDa, being consist of its predicted molecular weight. Although quantification of western blot demonstrated that the total *Ch*AMPK-α amount did not change obviously after compound C (CC) treatment in hemocytes (Fig. 9B), the level of Thr^{172} phosphorylation of *Ch*AMPK-α, which is considered as the activated marker of AMPK signaling, was significantly decreased after CC treatment when compared with the control group (Fig. 9C, $p < 0.05$). The ratios between Thr^{172} phosphorylation of *Ch*AMPK-α and total *Ch*AMPK-α were calculated (Fig. 9D). In the control group, the level of Thr^{172} phosphorylation of *Ch*AMPK-α was about 79.85% compared with 58.18% of the group treat with CC. Taken together, these results showed that compound C is one of the effective pharmacological molecular to suppress the AMPK signaling in the oyster.

3.6. Effects of compound C on phagocytosis and actin cytoskeleton

To investigate the effect of AMPK signaling on phagocytosis and actin cytoskeleton, the AMPK inhibitor CC has used since its availability was proved previously. Initially, the phagocytic ability of hemocytes was analyzed by the flow cytometery with EGFP-expressed bacteria. As showed in Fig. 10, the total phagocytic and adhesive rates decreased dramatically decreased from 32.37 ± 2.06% to 16.63 ± 2.27% after CC treatment ($p < 0.01$). However, the adhesion rates of control group and CC treatment group were only 2.67 ± 0.27% and 1.89 ± 0.36% without significant difference, strongly implying that AMPK signaling can affect the phagocytosis but not adhesion of oyster hemocytes.

Cytoskeleton remodeling is one target of AMPK signaling in the mammalian cells [31], so we test the whether the actin cytoskeleton could be changed by AMPK in oyster. The Phalloidin fluorescent dye was used to indicate the morphology of actin cytoskeleton. The results show the morphology of actin cytoskeleton changed dramatically after exposure to CC (Fig. 11). Fig. 11(B) and (C), (E)and (F) shows magnified region of interest. Normal actin fibres egin to disappear and deform and actin cytoskeleton collapsed into actin bundles. Notably, the actin filament could not stretch out and appear to be more turbulent than the control group, suggesting a crucial role in the organization of actin cytoskeleton. There results is strongly supported AMPK signaling could affect the actin cytoskeleton in the oyster hemocytes.

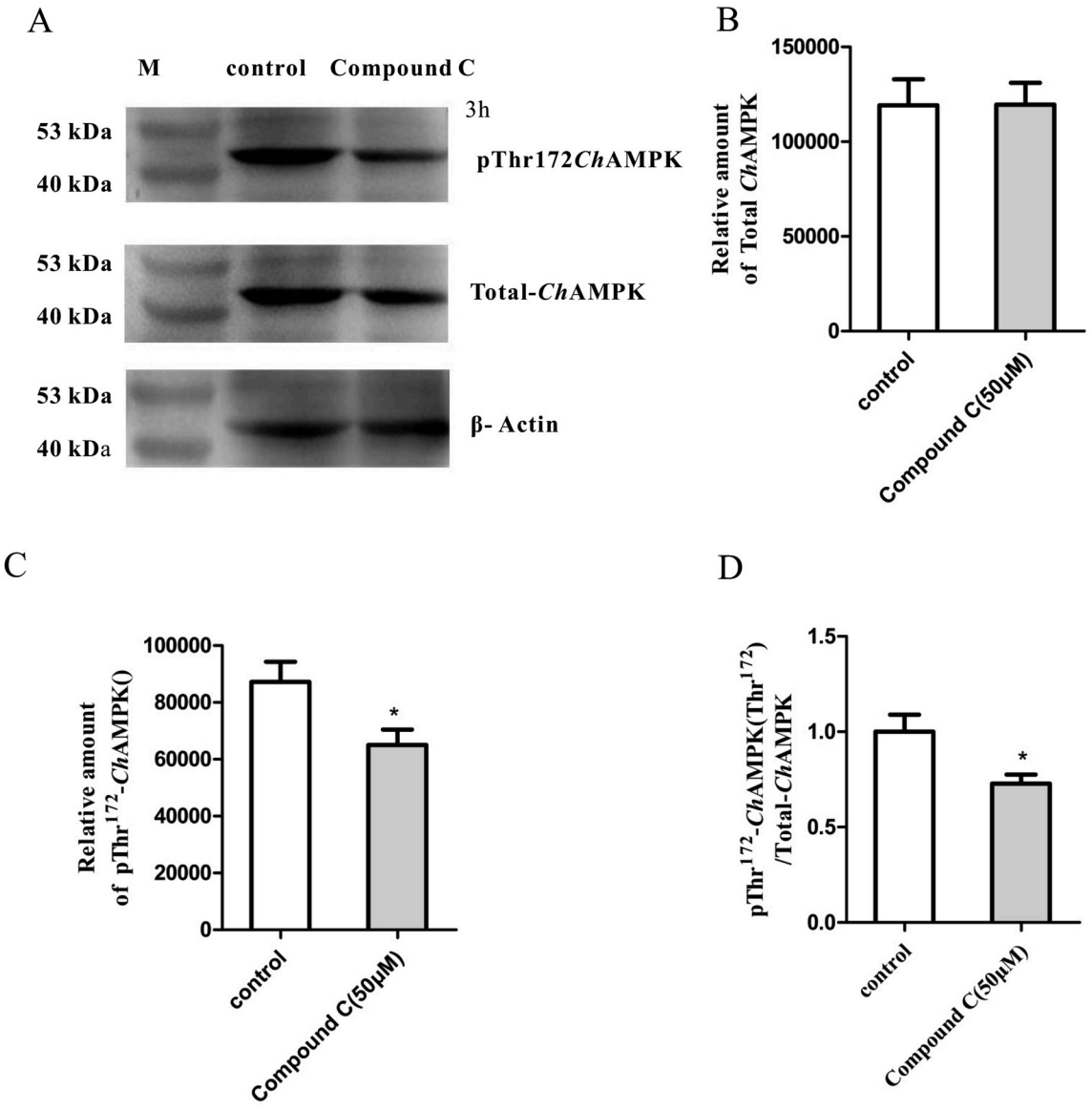

Fig. 9. Effects of Compound C on *Ch*AMPK protein. Effects of Compound C on *Ch*AMPK of hemocytes were cultured with Compound C (50 μM) for 3 h at 20 °C. Cell lysates were subjected to SDS-PAGE and Western blot analysis using specific antibodies for pThr^{172}*Ch*AMPK and total *Ch*AMPK. (A) shows representative image of Western blots. Quantification of total *Ch*AMPK(B), pThr^{172}*Ch*AMPK(C) and the ratio(D) were assessed by mean band optical density from 3 individual experiments (N = 3). (*, $p < 0.05$, **,$p < 0.01$, ***, $p < 0.001$).

4. Discussion

The function of AMPK has been well studied in vertebrates, but it is not clear whether AMPK has the same function in invertebrates. A recent study illustrates AMPK control cell polarity from invertebrates to mammals [34]. In rock crabs, a marine invertebrate, AMPK can be considered as an earlier indicator of temperature stress during the initial response to high temperatures [23]. In Pacific oyster, AMPK has been reported to be involved in maintaining aerobic metabolism in smooth muscle [35] and was ex-specifically regulated depending on gender in the gonad [36]. Our study identified three AMPK subunits from the HongKong oyster, namely *Ch*AMPK-α, *Ch*AMPK-β and *Ch*AMPK-γ, and explore the potential role of AMPK signaling in phagocytosis of hemocytes.

Sequence alignment and phylogenetic tree showed three subunits of AMPK are conserved cross from mollusk to mammals. Especially, the AMPK-α shared higher similarity of amino acid than *Ch*AMPK-β and *Ch*AMPK-γ, which may be due to catalytic function of the AMPK-α. Meanwhile, AMPK is directly activated by phosphorylation in the α subunit at Thr^{172} by upstream kinases, including LKB1, CaMKK, TAK1 and MLK3 [37]. By western blot analysis, Thr^{172}*Ch*AMPK-α could also be phosphorylated in the oyster hemocytes, implying the highly conserved activation of AMPK-α across multiple species. Therefore, pThr^{172}*Ch*AMPK-α could be as the activation state of AMPK-α in the oysters. Compound C (CC) is well-known for its potent inhibitory effect on AMPK activation in various human cells lines [38]. Here we found

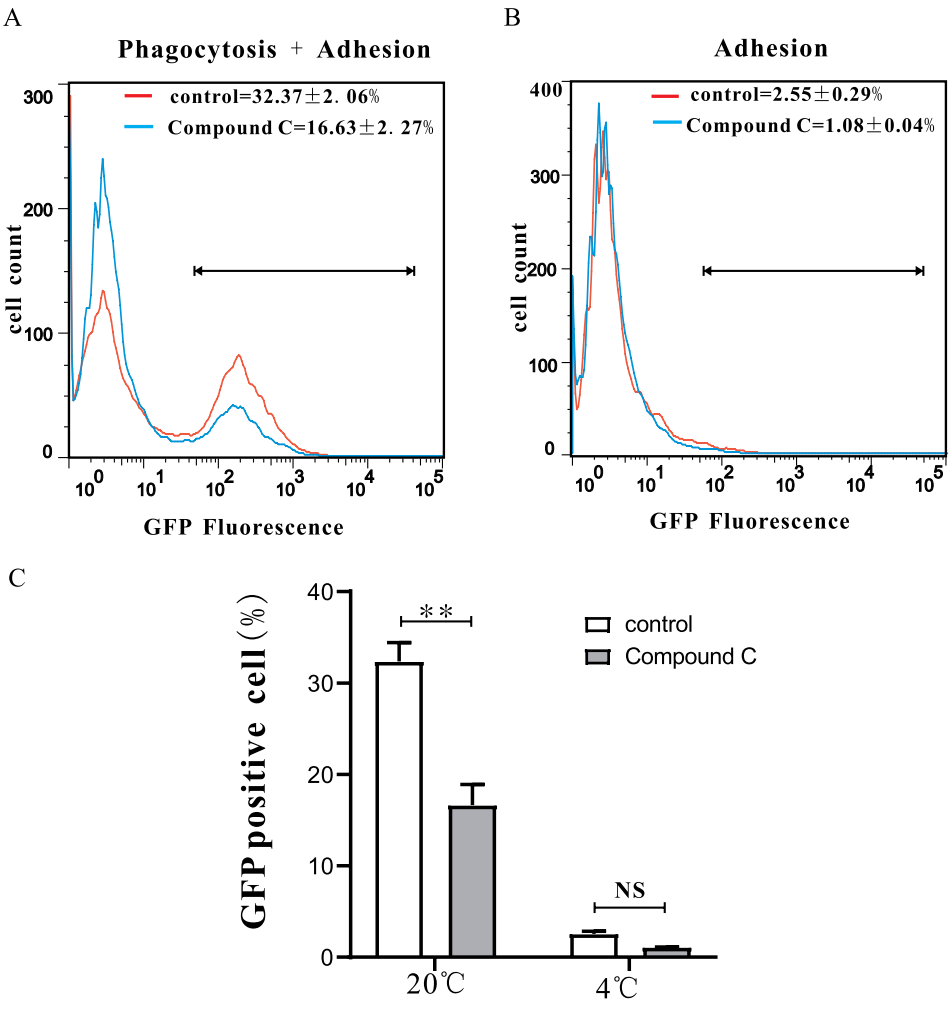

Fig. 10. Compound C attenuates phagocytosis of hemocytes. Red line and green line represent control group and experimental group respectively. (A)Representative images of flow cytometry analysis of phagocytosis and adhesion of hemocytes treated with Compound C at 20 ˚C. (B) Representative images of flow cytometry analysis of adhesion of hemocytes treated with Compound C at 4 ˚C. The GFP positive cells (C) of hemocytes. Data analysis was performed using GraphPad Prism 5 software and vertical bars represent the mean ± SE (N = 3), with *p < 0.05 and **p < 0.01. (For interpretation of the references to colour in this figure legend, the reader is referred to the Web version of this article.)

that CC can dramatically decrease the level of pThr^{172}*Ch*AMPK-α but not *Ch*AMPK-α, being consistent with the previous studies on macrophages and neutrophils [39,40]. Hence, these results demonstrate that CC could be one of powerful pharmacological tool to explore the function of AMPK in marine invertebrates.

The ability of phagocytes to engulf and ingest external pathogens, dead cells, or many other types of particles is a fundamental process in homeostasis and the immune in mullusk [41]. Previous studies showed that genetic or pharmacological inhibition of AMPK activity decreased macrophage phagocytosis [42]. As expected, treatment of CC could also suppress phagocytic ability to bacteria, but which cannot affect the bacterial adhesion of hemocyte, suggesting its role in control of phagocytosis is conserved from human to oyster. Moreover, multiple AMPK activators could also increase the phagocytic activity in macrophages [43], which also supports that the ability of phagocytosis is associated with AMPK activation.

Phagocytosis requires a conspicuous change in cell shape. Especially, the phagocytic cells have to deform to engulf particles that may represent a substantial fraction of its cellular size. Actin cytoskeleton, the major actor of cellular morphology, is the primary force driving phagocytosis [44]. Recently, the study showed that AMPK signaling activates phagocytosis via cytoskeletal reorganization, including enhancement of microtubule and actin polymerization [45]. We also observed that actin cytoskeleton is disordered and the actin filament is twist when AMPK signaling is inhibited in the hemocytes. Moreover, some studies also showed the present of positive feedback between AMPK signaling activation and actin cytoskeleton remodeling, since activation of AMPK was dependent on the later [46]. Actin is a central component of cytoskeleton filaments in eukaryotic cells, and its polymerization is required a lot of energy supply, such as ATP [47]. ATP could not only increase phagocytic rate but also improve microfilament bundles reorganization through changing F-actin structures [48]. As a key molecular sensor, AMPK signaling is crucial to maintain cellular energy homeostasis and intracellular ATP level [8,49], which could inevitably affect the phagocytosis and actin cyteskleton remodeling.

In summary, a novel molluscan AMPK homolog (*Ch*AMPK) was identified for the first time in *C. hongkongensis*. Results suggest that *Ch*AMPK is a member of the AMPK family and is homologous with the AMPK orthologs from other organisms. Moreover, the study gives clear insight that *Ch*AMPK is likely to be an essential regulator of the phagocytosis in the oysters via changing cytoskeleton and phosphorylation. These results could contribute to a better understanding of the phagocytosis of immune responses in an oyster. However, further studies are required for intensively illustrating a concrete mechanism for how the *Ch*AMPK regulates the phagocytosis.

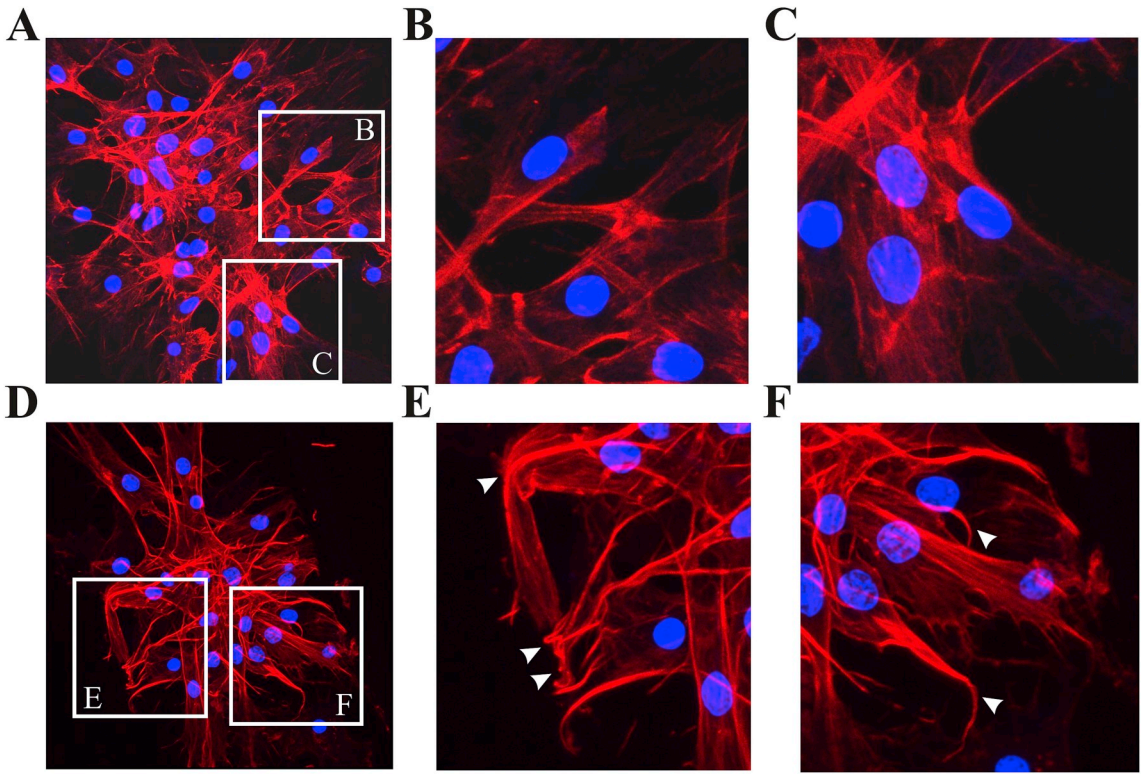

Fig. 11. AMPK modulates cytoskeleton remodeling. After treated with 50 μM compound C for 30 min and stained with DAPI and ActinRed, using laser scanning confocal microscopy to observe cytoskeleton. (A) and (D) is representative fluorescent merge images of control and CC treatment,respectively. (B), (C), (E)and (F) shows magnified region of interest.

Acknowledgments

This work was supported by the Guangdong Natural Science Funds for Distinguished Young Scholars (No.2015A030306003), the National Science Foundation of China (No. 31572640 and 31572661), the Guangdong Special Support Program of Youth Scientific and Technological Innovation (No. 2015TQ01N139), the Program of the Pearl River Young Talents of Science and Technology in Guangzhou of China (201806010003), Institution of South China Sea Ecology and Environmental Engineering, Chinese Academy of Sciences (No.ISEE2018PY03), Science and Technology Planning Project of Guangdong Province, China (2017B030314052, 201707010177).

References

[1] L. Zeng, B. Liu, C.W. Wu, J.L. Lei, M.Y. Xu, A.Y. Zhu, J.S. Zhang, W.S. Hong, Molecular characterization and expression analysis of AMPK α subunit isoform genes from Scophthalmus maximus responding to salinity stress, Fish Physiol. Biochem. 42 (6) (2016) 1595–1607.
[2] S.C. Lin, D.G. Hardie, AMPK: sensing glucose as well as cellular energy status, Cell Metabol. 27 (2) (2017).
[3] H.D. Grahame, AMP-activated protein kinase: a key system mediating metabolic responses to exercise, Med. Sci. Sport. Exerc. 36 (1) (2004) 28–34.
[4] D.G. Hardie, J.W. Scott, D.A. Pan, E.R. Hudson, Management of cellular energy by the AMP-activated protein kinase system, FEBS Lett. 546 (1) (2003) 113–120.
[5] H.D. Grahame, AMP-activated protein kinase: an energy sensor that regulates all aspects of cell function, Genes Dev. 25 (18) (2011) 1895–1908.
[6] H. Florian, S. Hanna, A.F. Popov, S. Christian, S. Julia, F. Martin, K.O. Coskun, V.L. Dirk, H. Jose, B. Martin, AMPK - activated protein kinase and its role in energy metabolism of the heart, Curr. Cardiol. Rev. 6 (4) (2010).
[7] D.S. Novikova, A.V. Garabadzhiu, G. Melino, N.A. Barlev, V.G. Tribulovich, AMP-activated protein kinase: structure, function, and role in pathological processes, Biochemistry 80 (2) (2015) 127–144.
[8] H.D. Grahame, S.A. Hawley, J.W. Scott, AMP-activated protein kinase–development of the energy sensor concept, J. Physiol. 574 (1) (2010) 7–15.
[9] M.A. David, P.G. Jesús Gustavo, G.G. Amelia, R.G. Lorena, S. Alfredo, C. Maria Roser, G. Mario, G. Borja, D. Cecilia, J.A.L. Calbet, Increased oxidative stress and anaerobic energy release, but blunted Thr172-AMPKα phosphorylation, in response to sprint exercise in severe acute hypoxia in humans, J. Appl. Physiol. 113 (6) (2012) 917–928.
[10] B.E. Crute, K. Seefeld, J. Gamble, B.E. Kemp, L.A. Witters, Functional domains of the alpha 1 catalytic subunit of the AMP-activated protein kinase, J. Biol. Chem. 273 (52) (1998) 35347–35354.
[11] S. Chen, AMPK Modulates Contractile Function of Cardiomyocytes, Dissertations & Theses - Gradworks (2014).
[12] J. Oakhill, J. Scott, Be, Structure and function of AMP-activated protein kinase, Acta Physiol. 196 (1) (2010) 3–14.
[13] D.G. Hardie, B.E. Schaffer, A. Brunet, AMPK: an energy-sensing pathway with multiple inputs and outputs, Trends Cell Biol. 26 (3) (2016) 190–201.
[14] M.M. Mihaylova, R.J. Shaw, The AMP-activated protein kinase (AMPK) signaling pathway coordinates cell growth, autophagy, & metabolism, Nat. Cell Biol. 13 (9) (2011) 1016.
[15] S.M. Jeon, Regulation and function of AMPK in physiology and diseases, Exp. Mol. Med. 48 (7) (2016) e245.
[16] J. Shuai, Z. Jia, Z. Tao, L. Wang, L. Qiu, J. Sun, L. Song, Functional characterisation of phagocytes in the Pacific oysterCrassostrea gigas, Peerj 4 (12) (2016).
[17] R.S. Flannagan, V. Jaumouillé, S. Grinstein, The cell biology of phagocytosis, Annu. Rev. Pathol. 7 (4) (2012) 61–98.
[18] S. Gordon, Phagocytosis: an immunobiologic process, Immunity 44 (3) (2016) 463–475.
[19] L. Wang, X. Song, L. Song, The oyster immunity, Dev. Comp. Immunol. 80 (2017).
[20] K.J. Ishii, S. Akira, Innate immune recognition of, and regulation by, DNA: trends in Immunology, Trends Immunol. 27 (11) (2006) 525–532.
[21] P. Dutta, T. Dey, A. Dihingia, P. Manna, J. Kalita, Antioxidant and glucose metabolizing potential of edible insect, Brachytrupes orientalis via modulating Nrf2/AMPK/GLUT4 signaling pathway, Biomed. Pharmacother. 95 (2017) 556–563.
[22] Z. Xiao-Jing, F. Chen-Zhuo, D. Zhong-Min, Z. Ruo-Chao, Y. Wei-Jun, AMPK alpha subunit gene characterization in Artemia and expression during development and in response to stress, Stress Int. J. Biol. Stress 10 (1) (2007) 53–63.
[23] F. Markus, M.R. O'Rourke, N.B. Furey, J.A. Jost, AMP-activated protein kinase (AMPK) in the rock crab, Cancer irroratus: an early indicator of temperature stress, J. Exp. Biol. 212 (Pt 5) (2009) 722.
[24] S.A. Stricker, Potential upstream regulators and downstream targets of AMP-activated kinase signaling during oocyte maturation in a marine worm, Reproduction 142 (1) (2011) 29–39.
[25] C.G. Goodchild, M. Frederich, S.I. Zeeman, AMP-activated protein kinase is a biomarker of energetic status in freshwater mussels exposed to municipal effluents, Sci. Total Environ. 512–513 (2015) 201–209.
[26] S. Xiao, N.-K. Wong, J. Li, Y. Lin, Y. Zhang, H. Ma, R. Mo, Y. Zhang, Z. Yu, Analysis of in situ transcriptomes reveals divergent adaptive response to hyper- and hypo-salinity in the Hong Kong oyster, Crassostrea hongkongensis, Front. Physiol. 9

(2018).
[27] F. Qu, Z. Xiang, F. Wang, Y. Zhang, J. Li, Y. Zhang, S. Xiao, Z. Yu, Identification and function of an evolutionarily conserved signaling intermediate in Toll pathways (ECSIT) from Crassostrea hongkongensis, Dev. Comp. Immunol. 53 (1) (2015) 244–252.
[28] Y. Zhang, X. Peng, Y. Liu, Y. Li, Y. Luo, X. Wang, H. Tang, Evaluation of suitable reference genes for qRT-PCR normalization in strawberry (Fragaria × ananassa) under different experimental conditions, BMC Mol. Biol. 19 (1) (2018) 8.
[29] X.Z.C.Z.H. Zhou, Synergistic antitumor activity of the combination of salubrinal and rapamycin against human cholangiocarcinoma cells, Oncotarget 7 (2016).
[30] D.W. Park, S. Jiang, J.M. Tadie, W.S. Stigler, Y. Gao, J. Deshane, E. Abraham, J.W. Zmijewski, Activation of AMPK enhances neutrophil chemotaxis and bacterial killing, Mol. Med. 19 (1) (2013) 387–398.
[31] M.T. van der Pauw, T. Van den Bos, V. Everts, W. Beertsen, Phagocytosis of fibronectin and collagens type I, III, and V by human gingival and periodontal ligament fibroblasts in vitro, J. Periodontol. 72 (10) (2001) 1340–1347.
[32] L. Ohman, G. Maluszynska, K.-E. Magnusson, O. Stendahl, Surface Interaction between Bacteria and Phagocytic Cells, (1988).
[33] L. Canesi, C. Pruzzo, R. Tarsi, G. Gallo, Surface Interactions between Escherichia coli and Hemocytes of the Mediterranean Mussel Mytilus galloprovincialis Lam. Leading to Efficient Bacterial Clearance, (2001).
[34] V. Mirouse, M. Billaud, The LKB1/AMPK polarity pathway, FEBS Lett. 585 (7) (2011) 981–985.
[35] E. Guévélou, A. Huvet, R. Sussarellu, M. Milan, X. Guo, L. Li, G. Zhang, V. Quillien, J.Y. Daniel, C. Quéré, Regulation of a truncated isoform of AMP-activated protein kinase α (AMPKα) in response to hypoxia in the muscle of Pacific oyster Crassostrea gigas, J. Comp. Physiol. B 183 (5) (2013) 597–611.
[36] G. Eric, H. Arnaud, C.E. Galindo-Sánchez, M. Massimo, Q. Virgile, D. Jean-Yves, Q. Claudie, B. Pierre, C. Charlotte, Sex-specific regulation of AMP-activated protein kinase (AMPK) in the Pacific oyster Crassostrea gigas, Biol. Reprod. 89 (4) (2013) 100.
[37] X. Liu, R.R. Chhipa, I. Nakano, B. Dasgupta, The AMPK inhibitor Compound C is a potent AMPK-independent anti-glioma agent, Mol. Cancer Ther. 13 (3) (2014) 596.
[38] H. Quan, Y.H. Hur, C. Xin, J.M. Kim, J.I. Choi, M.Y. Kim, H.B. Bae, Stearoyl lysophosphatidylcholine enhances the phagocytic ability of macrophages through the AMP-activated protein kinase/p38 mitogen activated protein kinase pathway, Int. Immunopharmacol. 39 (2016) 328–334.
[39] C. Blume, P.M. Benz, U. Walter, J. Ha, B.E. Kemp, T. Renne, AMP-activated protein kinase impairs endothelial actin cytoskeleton assembly by phosphorylating vasodilator-stimulated phosphoprotein, J. Biol. Chem. 282 (7) (2007) 4601–4612.
[40] S. Majd, S. Koblar, J. Power, Compound C enhances tau phosphorylation at Serine 396 via PI3K activation in an AMPK and rapamycin independent way in differentiated SH-SY5Y cells, Neurosci. Lett. 670 (2018) 53.
[41] A. Aderem, D.M. Underhill, Mechanisms of phagocytosis in macrophages, Annu. Rev. Immunol. 17 (17) (1999) 593–623.
[42] K.M. Jeong, J.I. Choi, S.H. Lee, H.J. Lee, J.K. Son, C.S. Seo, S.W. Song, S.H. Kwak, H.B. Bae, Effect of sauchinone, a lignan from Saururus chinensis, on bacterial phagocytosis by macrophages, Eur. J. Pharmacol. 728 (2014) 176–182.
[43] J.H. Ryu, B.D. Choi, C.W. Kim, C. Xie, D. Kang, J. Sung, M.K. Shin, N.G. Kim, S.K. Sang, Y.J. Choi, Aplysia kurodai-derived glycosaminoglycans increase the phagocytic ability of macrophages via the activation of AMP-activated protein kinase and cytoskeletal reorganization in RAW264.7 cells, J. Funct. Foods 27 (2016) 122–130.
[44] R.D. Labitigan, J.A. Theriot, Structure, dynamics, and mechanical forces: the actin cytoskeleton in neutrophil phagocytosis, Mol. Biol. Cell 28 (2017).
[45] H.B. Bae, J.W. Zmijewski, J.S. Deshane, J.M. Tadie, D.D. Chaplin, S. Takashima, E. Abraham, AMP-activated protein kinase enhances the phagocytic ability of macrophages and neutrophils, FASEB J. 25 (12) (2011) 4358–4368.
[46] V. Vivian, B. Phuong, E. Megumi, X. Aimin, S. Gary, Globular adiponectin induces LKB1/AMPK-dependent glucose uptake via actin cytoskeleton remodeling, J. Mol. Endocrinol. 51 (1) (2013) 155–165.
[47] J.W. Kuiper, H. Pluk, F. Oerlemans, F.N. van Leeuwen, L.F. De, J. Fransen, B. Wieringa, Creatine kinase-mediated ATP supply fuels actin-based events in phagocytosis, PLoS Biol. 6 (3) (2008) e51.
[48] G. Lu, Z. Lin, L. Zhou, Y. Han, G. Xu, Effects of atp on phagocytosis and microfilament bundles reorganization of macrophages, Acta Anat. Sin. 27 (1996).
[49] R. Lage, C. Diéguez, A. Vidal-Puig, M. López, AMPK: a metabolic gauge regulating whole-body energy homeostasis, Trends Mol. Med. 14 (12) (2008) 539–549.